

DETERMINATION ON INTERFACIAL FRACTURE TOUGHNESS OF THERMAL BARRIER COATINGS

Qi Zhu¹, Gaosheng Yan¹, Jianguo Zhu^{1*}, Wei He² and Daiheng Chen¹

¹ Faculty of Civil Engineering and Mechanics, Jiangsu University, Jiangsu, China, 212013

² AML, Department of Engineering Mechanics, Tsinghua University, Beijing, China, 100084

* Corresponding author. E-mail: zhujg@ujs.edu.cn

Keywords: Thermal barrier coatings, Three-point bending, Interfacial fracture toughness

ABSTRACT

A ceramic coating (topcoat) and a NiCoCrALY bondcoat were atmospheric-plasma-sprayed (APS) on a stainless steel substrate. A modified three-point bending test was adopted to initiate and propagate the topcoat/bondcoat (TC/BC) interfacial cracking. After a complete delamination, the fracture surfaces were examined by an optical microscope and a scanning electron microscope, which shows that the cracking plane was merely on the TC/BC interface. To obtain the crack length, the displacement and strain fields of the TC/BC cross-section were acquired using digital image correlation (DIC). Based on the experimental results, the critical strain energy release rate G_c for crack initiation was calculated with the Irwin-Kies formula, and the averaged magnitude was 152 J/m^2 . Moreover, the G_c for crack propagation was inversely determined by a finite element model to be in the range of $140\text{-}160 \text{ J/m}^2$. Good agreement between theoretical and numerical results is evidenced indicating that the two methods can be used for the evaluation of interfacial fracture toughness in thermal barrier coatings and other multi-layer structures.

1 INTRODUCTION

Thermal barrier coatings (TBCs) made of low-thermal conductivity ceramics are used to insulate metallic turbine and combustor engine components from the hot gas stream, and to improve their durability and energy efficiency. TBCs can protect a variety of structural engineering materials from corrosion, wear, and erosion, and provide lubrication and thermal insulation in aviation, shipping, nuclear, etc. Generally, TBC system is comprised of a superalloy substrate, a bondcoat (BC), and a ceramic topcoat (TC). During service, the demanding operating conditions could lead to an interfacial delamination of TBC. The spallation of the topcoat is one of the most serious issues among the premature failure modes, which can expose the bare metal to harsh environment. Moreover, the residual stresses arise during thermal spraying process could also result in a premature damage or failure, which is due to the remarkably different properties of each layer, such as the thermal expansion coefficient. Many experiments have revealed that the TBCs often fail from interfaces between TC and BC layers with the damage initiation and progression in the form of microcracks. Consequently, as an important property to analyze the as-deposited TBC failure, the interfacial fracture toughness of TC/BC is highly concerned recently, and various experimental methods have been proposed including tensile, shearing, buckling, indentation, and bending tests [1-10]. This work aims to develop a three-point bending test and to investigate the interfacial stress distribution and fracture toughness of TBC specimens.

2 EXPERIMENT

TBCs were prepared with the atmospheric plasma spraying. The substrate is SUS304 stainless steel with a dimension of $50 \times 5 \times 2 \text{ mm}^3$. The bondcoat material was NiCoCrAl with thickness of about $100 \mu\text{m}$ and the topcoat was yttrium oxide stabilized zirconia with thickness of about $200 \mu\text{m}$. Modified three-point bending specimens were fabricated as shown in Fig.1.

A monotonic load was applied to the specimen by a micro-mechanical testing machine. The tests were carried out under a constant displacement rate 0.05 mm/min at the loading point. The resolution of force and displacement was 1 N and 3 μm , respectively.

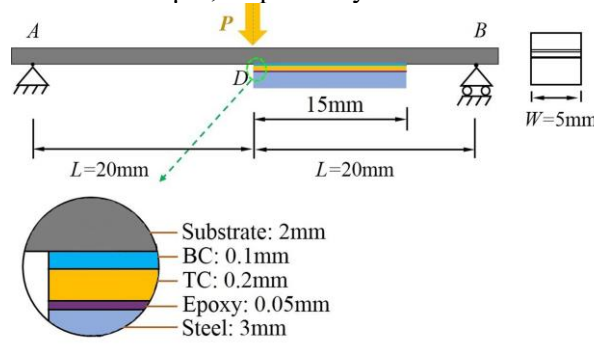


Figure 1: Specimen shape and size for three-point bending tests. Point D is supposed to be the crack initiation position.

3 CALCULATION

According to the Irwin-Kies formula, either under constant load or under constant displacement conditions, fracture toughness can be expressed in terms of the critical strain energy release rate G_c for a three-point bending beam as follows,

$$G_c = \left(\frac{P_c^2}{2W} \right) \left(\frac{\partial C}{\partial l} \right) \quad (1)$$

where P_c is the critical load when fracture occurs, W and l are the specimen width and crack length, respectively. The compliance of specimen, C , is expressed as

$$C = u / P \quad (1)$$

The compliance of each specimen can be obtained experimentally according to the relation between u and P .

Furthermore, inverse finite element analysis was resorted to determine the fracture energy. Finite element model was established to simulate the failure process of three-point bending test by using the commercial finite element analysis package (ABAQUS 6.10). A damage evolution law that describes the mixed mode fracture process of interface can be represented as

$$\left\{ \frac{\langle \sigma_n \rangle}{\sigma_n^0} \right\}^2 + \left\{ \frac{\langle \sigma_s \rangle}{\sigma_s^0} \right\}^2 = 1 \quad (3)$$

where the symbol $\langle \rangle$ represents the Macaulay bracket. Once the initiation criterion is reached, a damage evolution law that describes the mixed mode fracture process of interface can be represented as

$$\left(\frac{G_n}{G_{nc}} \right)^\alpha + \left(\frac{G_s}{G_{sc}} \right)^\alpha = 1 \quad (4)$$

where G_n and G_s are the work done by traction in normal and shear directions, respectively, and G_{nc} and G_{sc} are the required critical energies for interface fracture.

4 RESULTS

The load-displacement relationship of TBC specimens under mechanical tests is shown in Fig 2. The crack continues to propagate along the TC/BC interface after the crack initiation under the load of 161 N. Fig. 3(a) shows the interfacial delamination at the loading displacement of 0.410 mm. Digital image correlation (DIC) was used to precisely locate the crack tip with a magnified image of the

rectangular area (region of interest, ROI, Fig. 7(b)). Fig. 4 shows the curve of the crack-tip opening displacement along the interface when the loading displacement is 0.410 mm. In this way, the average crack length in relation to the different loading displacement was obtained, which will be used as the experimental data for fracture toughness calculation.

According to Eqs. (1) and (2), the values of fracture toughness of all the specimens were calculated. Take the specimen No. 1 as an example, the compliance was obtained by the ratio of u and P , and the relationship between C and l was shown in Fig. 5. By means of the least-square method, a linear fitting was used to obtain the value of $\partial C/\partial l$, which is $0.058 \mu\text{m}/\text{N}\cdot\text{mm}$. Finally, the calculated fracture toughness G_c was about $148\text{J}/\text{m}^2$. The fracture toughness of the five specimens is listed in Table 1. It can be seen that the experimental data has a good consistence, and the average value of fracture toughness G_c is about $154\text{J}/\text{m}^2$.

The fracture toughness was also calculated based on the finite element simulations. The total interfacial adhesion energy, G , was assumed to be between 40 and $200 \text{J}/\text{m}^2$. The numerical curve has the best agreement with experimental data when the interfacial adhesion energy is at the range of 140 - $160 \text{J}/\text{m}^2$, as shown in Fig. 6.

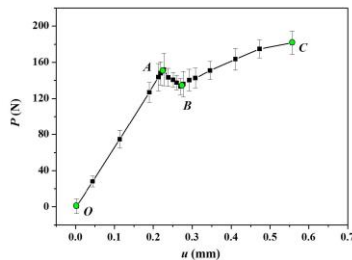


Figure 2: Load-displacement relationship of TBC specimens.

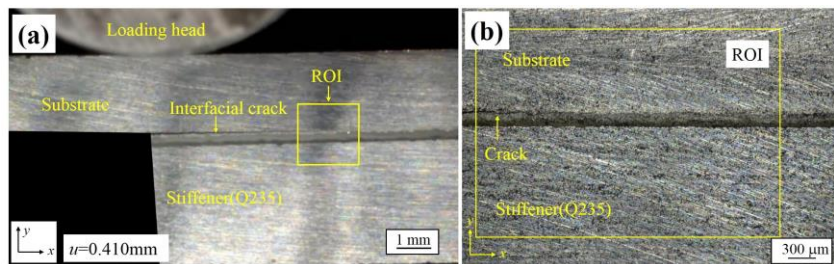


Figure 3: (a) Cross-sectional image of specimen with loading displacement of 0.410 mm. (b) Magnified image of the rectangle area in the yellow box at the crack tip.

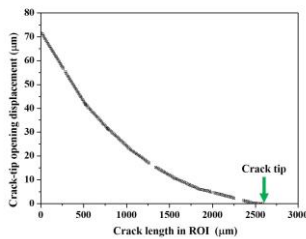


Figure 4: Relationship curve of crack-tip opening displacement and the crack length in ROI.

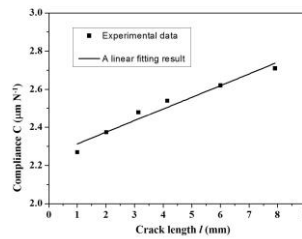


Figure 5: Compliance versus crack length of TBC (specimen No. 1).

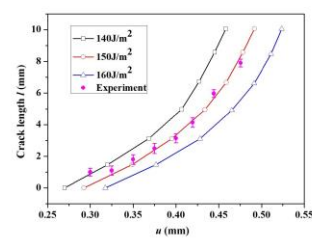


Figure 6: Relationship curves of crack length and loading displacement.

Specimen No.	$P_c(\text{N})$	$\partial C/\partial l$ ($\mu\text{m}/\text{N}\cdot\text{mm}$)	G_c (J/m^2)
1	160	0.058	148.48
2	149	0.060	147.89
3	172	0.054	159.75
4	165	0.057	155.18
5	161	0.061	158.18
Average	161	0.058	153.90

Table 1 Critical energy release rate G_c of TBC specimens.

5 CONCLUSIONS

A modified three-point bending test combined with digital image correlation method has been

proposed for the determination of critical adhesion energy. Based on the Irwin-Kies formula and finite element model, the critical adhesion energies of the initiation and propagation of the TC/BC interfacial crack were calculated, and their values are 152 J/m² and 140-160 J/m², respectively. Good agreement between the theoretical and numerical results has been obtained, which indicates that the two methods can be used for the evaluation of interfacial fracture toughness in thermal barrier coatings and other multi-layer structures.

ACKNOWLEDGEMENTS

The authors are grateful for the financial support from the National Natural Science Foundation of China (Grant Nos. 11232008, 11372118) and the Natural Science Foundation of Jiangsu Province, China (Grant No. BK20161341).

REFERENCES

- [1] G. Qian, T. Nakamura, C.C. Berndt, S.H. Leigh, G. Qian, T. Nakamura, C.C. Berndt, S.H. Leigh, Tensile toughness test and high temperature fracture analysis of thermal barrier coatings, *Acta Materialia*, **45**, 1997, pp.1767-1784.
- [2] S.S. Kim, Y.F. Liu, Y. Kagawa, Evaluation of interfacial mechanical properties under shear loading in EB-PVD TBCs by the pushout method, *Acta Materialia*, **55**, 2007, pp. 3771-3781.
- [3] Z.H. Xu, Y. Yang, P. Huang, X. Li, Determination of interfacial properties of thermal barrier coatings by shear test and inverse finite element method, *Acta Materialia*, **58**, 2010, pp. 5972-5979.
- [4] W. Zhu, L. Yang, J.W. Guo, Y.C. Zhou, C. Lu, Determination of interfacial adhesion energies of thermal barrier coatings by compression test combined with a cohesive zone finite element model, *International Journal of Plasticity*, 2014, pp. 76–87.
- [5] Q. Chen, W.G. Mao, Y.C. Zhou, C. Lu, Effect of Young's modulus evolution on residual stress measurement of thermal barrier coatings by X-ray diffraction, *Applied Surface Science*, **256**, 2010, pp. 7311-7315.
- [6] W. Mao, C. Dai, L. Yang, Y. Zhou, Interfacial fracture characteristic and crack propagation of thermal barrier coatings under tensile conditions at elevated temperatures, *International Journal of Fracture*, **151**, 2008, pp. 107-120.
- [7] T.T. Y. C. Zhou, A. Yoshida, L. Liu, G. Bignall Fracture characteristics of thermal barrier coatings after tensile and bending tests, *Surface & Coatings Technology*, **157**, 2002, pp. 118.
- [8] I. Hofinger, M. Oechsner, H.A. Bahr, M.V. Swain, Modified four-point bending specimen for determining the interface fracture energy for thin, brittle layers, *International Journal of Fracture*, **92**, 1998, pp. 213-220.
- [9] Y. Yamazaki, A. Schmidt, A. Scholz, The determination of the delamination resistance in thermal barrier coating system by four-point bending tests, *Surface & Coatings Technology*, **201**, 2006, pp. 744-754.
- [10] P.F. Zhao, C.A. Sun, X.Y. Zhu, F.L. Shang, C.J. Li, Fracture toughness measurements of plasma-sprayed thermal barrier coatings using a modified four-point bending method, *Surface & Coatings Technology*, **204**, 2010, pp. 4066-4074.